

## **Biosynthesis of Pd Nanoparticle Using Onion Extract for Electrochemical Determination of Carbendazim**

Dan Liu, Fengzhi Wu\*

Department of Horticulture, Northeast Agricultural University, Harbin 150030, China

\*E-mail: [fzwu2006@aliyun.com](mailto:fzwu2006@aliyun.com)

*Received:* 19 December 2016 / *Accepted:* 28 January 2017 / *Published:* 12 February 2017

---

Recently, nanomaterials through biosynthesis have attracted extensive attention, owing to their non-toxic approaches. Herein, an environmental-friendly chemical approach was proposed to photo-synthesize palladium nanoparticles (Pd NPs) with the extract of onion. UV-Vis spectroscopy, FTIR, SEM and XRD were employed to analyze the bio-synthesized Pd NPs. According to SEM as well as dynamic light scattering instrument, the mean size of the bio-synthesized Pd NPs was measured to be 18.9 nm. Furthermore, the bio-synthesized Pd NPs was used to modify the surface of the screen-printed electrode, which exhibited an outstanding electro-catalytic activity for the determination of carbendazim in soil.

---

**Keywords:** Pd NPs; Biosynthesis; Onion; Electrochemistry; Sensing; Carbendazim

### **1. INTRODUCTION**

Nanoscience and nanotechnology have received wide attentions during the past two decades, where the base of nanotechnology is to produce the desired nanostructures [1]. Nanomaterials is a term of material, which at least possess one dimension in the range of 1-100 nm. Numerous materials with diverse morphology have been prepared. In particular, the metallic nanomaterials have received massive attentions in various areas because of their inherent properties compared to their bulk state [2]. Besides, the chemical, physical and mechanical properties of the metallic nanomaterials could be tuned through their surface area, size and size distribution as well as the dispersion status. Normally, the metallic nanomaterials exhibited high specific surface area. Hence, they are favorable in various applications including sensor, catalysis and anti-bacteria [3]. So far, numerous metallic nanostructures, including copper [4], gold, [5] palladium, [3] platinum [6] and silver [7], have been produced through the well-defined chemical approaches.

The synthesis of Pd NPs has obtained numerous attentions due to their distinct chemical, physical, thermodynamic as well as optical characteristics in nanoscale [8]. Hence, Pd NPs have been widely applied in the area of surface-enhanced Raman spectroscopy (SERS) [9], catalysis [10] drug delivery [11]. By far, diverse wet-synthesis methods have been employed to synthesize Pd NPs with various sizes and morphologies, including polyols [12], chemical [13], and sonochemical [14] reduction. In general, these wet-synthesis methods are facile and exhibited high growth rate as well as high yield. Nevertheless, hazardous chemicals have been widely used in these approaches, which has raised severe attention on the potential side effects of the chemical-synthesized metal nanoparticles towards the living and environment. Thus, to develop green-chemistry methods, which are nontoxic as well as ecofriendly, are of great importance.

The bio-fabrication of the metal nanoparticles, which is an environment-friendly method, has attracted remarkable attention recently due to its mild experimental conditions including pH, pressure and temperature [15]. Because of the advantages of the biofabricated metal nanoparticles described above, researchers have focus on the synthesis of Pd NPs through bio-fabrication and their applications. However, the bio-fabrication of Pd NPs is still in the primary status. Only few reports have employed biological sources to synthesize and stabilize Pd NPs, such as the peel extract of *Annona squamosa* (sugar-apple) [16], the extract of *Cinnamom zeylanicum* (cinnamon) bark [17], the peel extract of *Musa paradisiaca* (banana) [18] and leaf extract of *Anacardium occidentale* (cashew nut) [19]. Nowadays, Pd NPs through biosynthesis have been investigated for diverse applications, such as catalyst for Heck reaction [20] and decolorization of azo dyes [21]. Thus, to explore the catalytic performance of Pd NPs towards diverse biological and environmental applications is remarkably promising.

Herein, a new biosynthesis approach was proposed to prepare Pd NPs with the extract of onion as the reductant. Various techniques were employed to characterize the morphology and determine properties of the as-prepared Pd NPs. Furthermore, the as-prepared Au NPs also exhibited a remarkable electrochemical performance for the detection of carbendazim (methyl 1H-benzimidazol-2-ylcarbamate).

## 2. EXPERIMENT DETAIL

### 2.1. Materials

All the chemicals, which were analytically pure, were commercially available (Sigma-Aldrich). For all the experiments, Milli-Q water was employed. Onion (*Allium cepa* L) was bought in local supermarket, which was then rinsed with water to remove external impurity. After being dried, the onion was cut into small pieces and smashed with a blender in the presence of water. After filtration, the extract of onion was collected and then dried to obtain the extract powder in oven.

## 2.2. Biosynthesis of Pd NPs using Onion extract

PdCl<sub>2</sub> and the extract of onion was used to biosynthesize Pd NPs as the precursor for Pd and reductant, respectively. In general, the extract of onion (0.5 g) was added into 20 mL PdCl<sub>2</sub> with a concentration of 10 mM under sonication for 2h. The color of solution varied from pale yellow to black, which indicated that Pd NPs was generated. After that, the solution was centrifuged and rinsed with water to remove the excess extract of onion. Then the residue was dried to obtain the bio-synthesized Pd NPs.

## 2.3. Characterizations of biosynthesized Pd NPs

SEM (ZEISS X-MAX) was used to characterize the morphology of the bio-synthesized Pd NPs. XRD (D8-Advance) was employed to record the crystal pattern of the bio-synthesized Ag NPs in the range of 10° to 80° in 2θ. Furthermore, UV-Vis spectroscopy (Shimadzu UV-1601PC) was utilized to analyse the optical property of the bio-synthesized Ag NPs. A CHI 660 electrochemical workstation (CH Instruments, USA) was employed to perform all electrochemical determination. Fourier transform infrared spectra (FTIR) were acquired from a Bruker Vertex 70 spectrometer.

## 2.4. Electrochemical characterization

The three-electrode system was employed to electrochemically determine carbendazim, where the screen-printed electrode (SPE) modified with the biosynthesized Pd NPs, Pt foil and saturated Ag/AgCl were used as working electrode, counter electrode and reference electrode, respectively. The modification of the SPE surface was performed according to the following process: the suspension of Pd NPs (0.1 mL) with a concentration of 1mg/mL was deposited on the surface of SPE and then dried at room temperature. The surface electron-transfer capacity of the electrode was analysed through electrochemical impedance spectroscopy (EIS) with and without modification. In this work, [Fe(CN)<sub>6</sub>]<sup>3-/4-</sup> (5 mM) and KCl (0.1 M) were used as probe and supporting electrolyte, respectively. The frequency ranged from 10<sup>1</sup> to 10<sup>5</sup> Hz, where the amplitude was set to be 5 mV. CV method was employed to carry out the determination of carbendazim in PBS (0.1M) with a pH of 7, where the scan range was from 0 to 1.0 V with a scan rate of 50 mV/s.

## 2.5. Soil sample analysis

SPE modified with the bio-synthesized Pd NPs was employed to detect carbendazim in the soil specimen. To be specific, the mixture of ethylene glycol and choline chloride (500μL) was added into soil sample (1 g) placed in a Petri dish. 15 min later, the Pd NPs-based SPE was inserted into the soil specimen. The linear sweep voltammetry (LSV) approach was employed into the analytical determination. Besides, the standard addition was also used to determine carbendazim in the soil specimens.

### 3. RESULT AND DISCUSSION

The visual color change during the experiment confirmed that Pd NPs was successfully generated. SEM was employed to characterize the morphology of Pd NPs. In Figure 1, a small cluster with spherical shape was observed with the bio-synthesized Pd NPs. Because of the biomolecules present on the surface of Pd NPs, the observed aggregation was negligible. It was obvious that the as-synthesized Pd NPs exhibited a solid structure with a mean diameter of 18.9 nm through measuring around 100 Pd NPs.

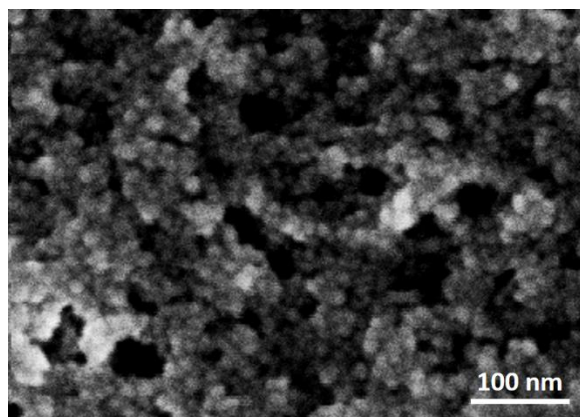


**Figure 1.** SEM image of the bio-synthesized Pd NPs.

Pd NPs was fabricated with the extract of onion and monitored visually and further with UV-Vis spectroscopy (Figure 2). The color of the reaction gradually changed to dark brown from yellow during the process of visual monitoring, which was induced by the excitation of the surface plasmon resonance of Pd NPs. As shown in the UV-visible spectrum of the mixed PdCl<sub>2</sub> solution, a distinct peak emerged at 300 nm which can be ascribed to the Pd<sup>2+</sup> ions.

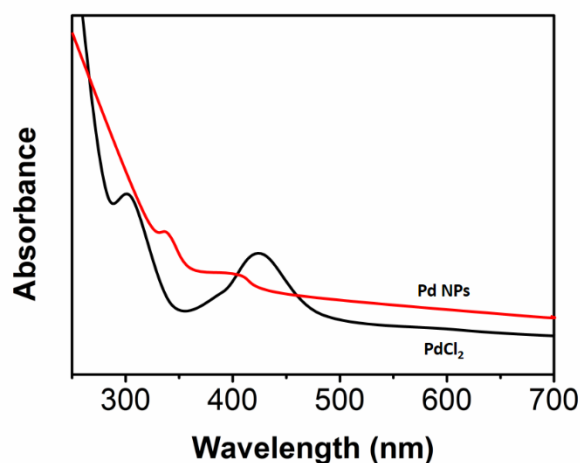


**Figure 2.** UV-visible spectrum of PdCl<sub>2</sub> solution (0.5 mM, pH=3) and biosynthesized Pd-NPs in the onion extract.

With the formation of Pd NPs, this peak gradually decreased and finally disappeared during the reaction time of 3 h, while an absorption band that was assigned to Pd NPs was observed in the spectrum. This suggests that the Pd<sup>2+</sup> ions were reduced to the metal Pd<sup>0</sup>. In addition, a continuous absorption spectrum shifted from the visible region to ultraviolet region with an increase in intensity. This indicates that a complete reduction of Pd<sup>2+</sup> ions to the metal Pd<sup>0</sup> was achieved.

FTIR was carried out to analyze the functional groups on the surface of biosynthesized Pd NPs, and results were showed in Figure 3A. As it can be seen, several peaks emerged at 660 (alkene C–H band), 695 ((NH) C=O group of cyclic peptides), 1033 (C–N stretching vibration of aliphatic amines), 1642 (N–H band of primary amines), 2954 (C–H stretching vibration of alkanes amide) and 3403 cm<sup>-1</sup> (O–H group in alcohols and phenols). Owing to the existence of these functional groups on the surface, the stability of Pd NPs can be highly enhanced. Furthermore, according to the reported literatures, the presence of amino acids, carbohydrates, fatty acids, minerals, phenolic compounds, and vitamins are contributed to the reduction of PdCl<sub>2</sub> [22-24]. Here, as a reducing agent, the cyclic peptides can also reduce Pd<sup>2+</sup> ions to the metal Pd<sup>0</sup>.

X-ray diffraction was used to characterize the crystal structure of biosynthesized Pd NPs. As shown in Figure 3B, the XRD patterns of the biosynthesized Pd NPs, a series of diffraction peaks emerged at 36.58°, 43.09°, 64.82° and 77.63° which are ascribe to the (200), (220), (311) and (222) of fcc (face-centered-cube) silver (JCPDS 04-0783), respectively. In addition, no additional diffraction peaks were observed in the pattern. This suggests that the biosynthesized Pd NPs were pure. Based on the Debye-Scherrer equation:  $D = 0.9\lambda / \beta \cos \theta$ , where D,  $\lambda$ ,  $\beta$ ,  $\theta$  are represented as the crystalline size, X-ray wavelength, full width at half of the maximum intensity peak, Bragg's angle, respectively, the crystallite size of Pd NPs was calculated to be 11.5 nm.

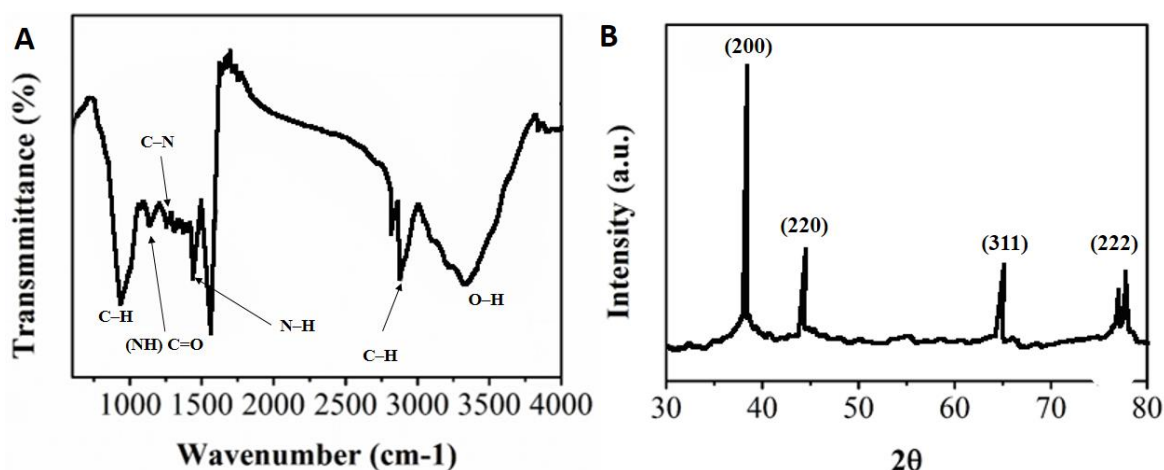


**Figure 3.** (A) FTIR and (B) XRD results of biosynthesized Pd NPs.

Although the biosynthesis mechanism of the Pd NPs is unknown, it can be deduce that the polyol compounds maybe important for the reduction of Pd<sup>2+</sup> to Pd NPs according to the detected strong reducing ability of polyol compounds [25, 26]. There are two hydroxyl groups in the gallic acid that might play an important role in the reduction of Pd<sup>2+</sup>. Normally, phenolic compounds can easily

donate electrons and thus be oxidized into quinones form. Herein, in the reduction process of  $\text{PdCl}_2$ , the gallic acid probably firstly formed an intermediate with palladium species. Then, gallic acid was oxidized to its quinone form accompanying with the formation of nascent hydrogen or free electrons. Subsequently,  $\text{Pd}^{2+}$  ions were reduced to  $\text{Pd}^0$  by the free electron or nascent hydrogen. Finally, resulted in the collision and stacking of formed  $\text{Pd}^0$  atoms, Pd NPs were gradually generated.

For evaluating the modification of electrode surface, EIS is one of the useful strategies, since the semicircle part obtained in Nyquist plot at high frequencies is helpful for the determination of charge transfer limiting process. The spectra of bare SPE and Pd NPs modified SPE were recorded in Figure 4A. Pd NPs modified SPE was measured in a solution containing KCl (0.1 M) and  $[\text{Fe}(\text{CN})_6]^{3-/4-}$  (5 mM). Bare SPE shows a charge transfer resistance value of 698  $\Omega$ . In contrast, owing to the excellent electronic property of Pd NPs, this value of SPE increased significantly after modified by Pd NPs.

CV (cyclic voltammograms) were employed to perform electrochemical properties of bare SPE and Pd modified SPE by using  $[\text{Fe}(\text{CN})_6]^{3-/4-}$  as an electrochemical probe, and results were collected in Figure 4B. Both bare SPE and Pd NPs modified SPE were measured in KCl (0.1 M) and  $[\text{Fe}(\text{CN})_6]^{3-/4-}$  (5 mM) with a scan rate of 100 mV/s. As shown, a pair of reversible redox peaks were observed in the CV of bare SPE that are attributed to the one-electron transfer process of  $\text{Fe}(\text{CN})_6^{3-/4-}$ . In the case of Pd NPs modified SPE, the redox current increased significantly, because the conductivity and surface area of Pd NPs modified SPE are superior to that of bare SPE.

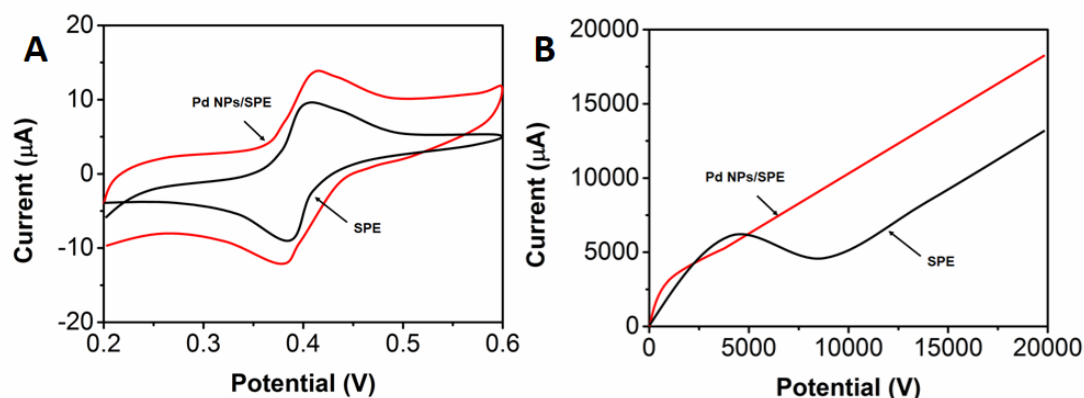


**Figure 4.** (A) CV of bare SPE and Pd NPs modified SPE, (B) Nyquist curves of bare SPE and Pd NPs modified SPE measured in a solution containing KCl (0.1 M) and  $[\text{Fe}(\text{CN})_6]^{3-/4-}$  (5 mM).

The electrochemical behaviors of bare SPE and Pd NPs modified SPE were evaluated with pesticide containing carbendazim (0.1 mM), and results were diagrammed in Figure 4. The bare SPE only shows a weak reduction peak that is related to the reduction of nitric group in carbendazim. In the case of Pd NPs modified SPE, the reduction peak current is higher than that of bare SPE. This may be also caused by the superior conductivity and surface area of Pd NPs modified SPE. In addition, an obvious shift of reduction peak to positive direction was obtained, which reveals that the modification

by Pd NPs can further decrease the reduction over potential. And thus it shows an excellent electrocatalytic activity towards carbendazim.

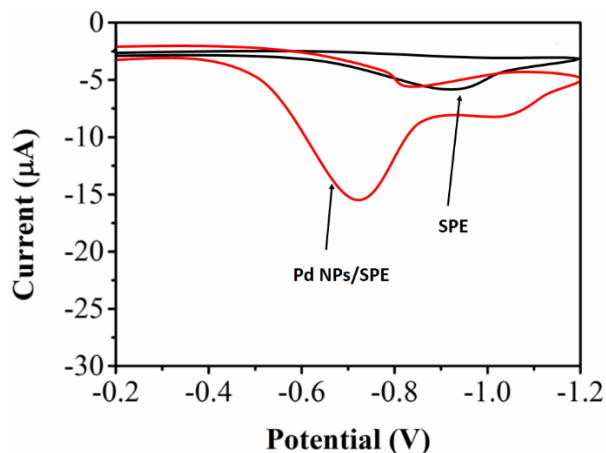


**Figure 5.** CV of bare SPE and Pd NPs modified SPE for 100  $\mu\text{M}$  carbendazim in PBS ( $\text{pH} = 7$ ) with a scan rate of 50 mV/s.

In Figure 6, the amperometric response of the Pd NPs modified SPE as a function of carbendazim concentration was also investigated. Obviously, the amperometric response of Pd NPs/SPE was present and reached to the steady-state in 4 s soon after the addition of the carbendazim. In the inset of Figure 6A, the obtained Pd NPs/SPE sensor shows a linear response of currents vs. the carbendazim concentrations in the range from 0.02  $\mu\text{M}$  to 35  $\mu\text{M}$ . Moreover, the detection limit was detected equal to 3 nM on the basis of signal to noise ratio of 3. For comparison, the performances of a group of reported sensor and obtained electrochemical carbendazim sensor in this work were listed in Table 1. It shows that the Pd NPs modified SPE possesses a comparable performance for the determination of carbendazim.

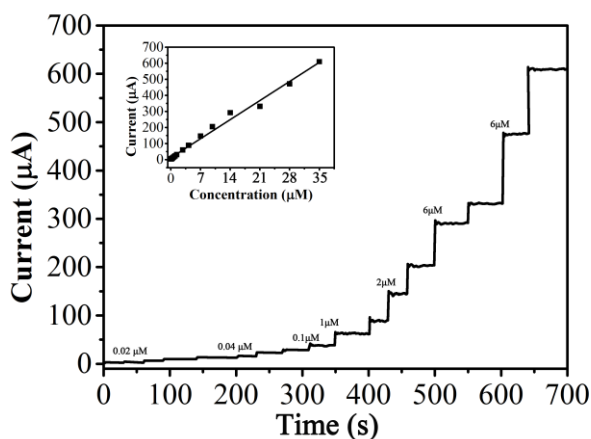


**Figure 6.** Amperometric response of the Pd NPs/SPE vs. carbendazim concentration in PBS under the condition of 0.71 V. Inset: current respond against to carbendazim concentration in the range from 0.02 to 35  $\mu\text{M}$ .

**Table 1.** Comparison of obtained electrochemical carbendazim sensor with other reported sensors.

Electrode	LDR ( $\mu\text{M}$ )	LOD ( $\mu\text{M}$ )	Reference
Biosynthesized Au/SPE	0.05-25	0.0029	[27]
Carboxylic group functionalized poly(3,4-ethylenedioxythiophene)	7-45	2.2	[28]
SiO <sub>2</sub> /MWCNT	0.2-4	0.056	[29]
Reduced N-doped GO/GCE	0.5-40	0.1	[30]
Boron-doped diamond anode	0.02-5	0.01	[31]
Phosphorus-doped helical carbon nanofibers	0.02-9	0.01	[32]
Graphene-based electrochemical sensor	0.5-50	0.1	[33]
GO-MWNTs hybrid nanomaterial	0.2-0.5	0.15	[34]
Biosynthesized Pd/SPE	0.02-35	0.003	This work

The obtained Pd NPs modified SPE was utilized to analyze the carbendazim with a trace amount in two soil samples which are collected from the cultivated land as real environmental samples. The results of carbendazim content determination in these two soil samples were showed in Table 2. As shown, the Pd NPs modified SPE has an excellent performance of carbendazim detection for soil samples. Thus, the obtained Pd NPs modified carbendazim sensor can be applied to the detection of carbendazim in real environmental samples.

**Table 2.** Results of carbendazim detection in soil samples using Pd NPs modified SPE.

Sample	Added ( $\mu\text{M}$ )	Found ( $\mu\text{M}$ )	Recovery (%)
Soil sample 1	0	0	—
	0.5	0.504	100.8
	2	2.101	105.1
	5	4.985	99.7
Soil sample 2	0	0.011	—
	0.1	0.120	108.1
	0.2	0.219	103.8
	0.7	0.732	103.0

#### 4. CONCLUSION

In the present work, we reported a biosynthesis strategy of preparing Pd nanoparticles using a reducing agent of onion extract. Pd NPs with spherical morphology were synthesized, and the average diameter of Pd NPs is equal to 18.9 nm. Obtained Pd NPs modified SPE shows good electrocatalytic performance towards the detection of carbendazim. The linear relationship was obtained in the detection region of 0.052-35  $\mu\text{M}$ . And the detection limit of obtained carbendazim sensor is 3 nM. In addition, the proposed electrochemical carbendazim sensor can be successfully applied to the determination of carbendazim in real environmental samples.

## References

1. R.W. Raut, A.S.M. Haroon, Y.S. Malghe, B.T. Nikam and S.B. Kashid, *Adv. Mat. Lett.*, 4 (2013) 650.
2. A. Viswadevarayalu, P.V. Ramana, J. Sumalatha and S.A. Reddy, *J.Nanosci. Tech.*, (2016) 169.
3. K. Anand, C. Tiloke, A. Phulukdaree, B. Ranjan, A. Chuturgoon, S. Singh and R. Gengan, *J. Photoch. Photobio. B*, 165 (2016) 87.
4. M.K. Ahmadi, M. Ghafari, J.D. Atkinson and B.A. Pfeifer, *Chem. Eng. J.*, 306 (2016) 772.
5. A. Malhotra, K. Dolma, N. Kaur, Y. Rathore, S. Mayilraj and A.R. Choudhury, *Bioresour. Technol.*, 142 (2013) 727.
6. D. Chen, C. Zhao, J. Ye, Q. Li, X. Liu, M. Su, H. Jiang, C. Amatore, M. Selke and X. Wang, *ACS Appl. Mater. Interfaces*, 7 (2015) 18163.
7. S.A. Shafiq, R.H. Al-Shammari and H.Z. Majeed, *International Journal of Innovation and Applied Studies*, 15 (2016) 43.
8. K. Watanabe, D. Menzel, N. Nilius and H.-J. Freund, *Chem. Rev.*, 106 (2006) 4301.
9. H. Chen, G. Wei, A. Ispas, S.G. Hickey and A. Eychemüller, *J. Phys. Chem. C.*, 114 (2010) 21976.
10. R. Chen, Y. Jiang, W. Xing and W. Jin, *Ind. Eng. Chem. Res.*, 52 (2013) 5002.
11. P. Ghosh, G. Han, M. De, C. Kim and V. Rotello, *Adv. Drug Delivery Rev.*, 60 (2010) 1307.
12. C. Nieto-Oberhuber, S. López, M.P. Munoz, D.J. Cárdenas, E. Buñuel, C. Nevado and A.M. Echavarren, *Angew. Chem., Int. Ed.*, 117 (2005) 6302.
13. K.A. Flanagan, J.A. Sullivan and H. Müller-Bunz, *Langmuir*, 23 (2007) 12508.
14. A. Nemamcha, J.-L. Rehspringer and D. Khatmi, *J. Phys. Chem. B.*, 110 (2006) 383.
15. P. Dauthal and M. Mukhopadhyay, *Ind. Eng. Chem. Res.*, 52 (2013) 18131.
16. S.M. Roopan, A. Bharathi, R. Kumar, V.G. Khanna and A. Prabhakarn, *Colloids Surf., B*, 92 (2012) 209.
17. M. Sathishkumar, K. Sneha, I.S. Kwak, J. Mao, S. Tripathy and Y.-S. Yun, *J. Hazard. Mater.*, 171 (2009) 400.
18. A. Bankar, B. Joshi, A.R. Kumar and S. Zinjarde, *Mater. Lett.*, 64 (2010) 1951.
19. D. Shen, D. Philip and J. Mathew, *Spectrochim. Acta, Part A*, 91 (2012) 35.
20. P. Zhou, H. Wang, J. Yang, J. Tang, D. Sun and W. Tang, *Ind. Eng. Chem. Res.*, 51 (2012) 5743.
21. L. Xu, X.-C. Wu and J.-J. Zhu, *Nanotechnology*, 19 (2008) 305603.
22. J.-I. Yang, C.-C. Yeh, J.-C. Lee, S.-C. Yi, H.-W. Huang, C.-N. Tseng and H.-W. Chang, *Molecules*, 17 (2012) 7241.
23. K. Satyavani, S. Gurudeeban, T. Ramanathan and T. Balasubramanian, *J. Nanobiotechnol.*, 9 (2011) 2.
24. S. Kansal, M. Singh and D. Sud, *J. Hazard. Mater.*, 153 (2008) 412.
25. N. Asano, T. Yamashita, K. Yasuda, K. Ikeda, H. Kizu, Y. Kameda, A. Kato, R.J. Nash, H.S. Lee and K.S. Ryu, *J. Agric. Food Chem.*, 49 (2001) 4208.
26. C. Proestos, N. Choriantopoulos, a. G.J. E. Nychas and M. Komaitis, *J. Agric. Food Chem.*, 53 (2005) 1190.
27. L. Li, Z. Zhang, *Int. J. Electrochem. Sc.*, 11 (2016) 4550.
28. Y. Yao, Y. Wen, Z. Long, Z. Wang, Z. Hui and J. Xu, *Anal. Chim. Acta.*, 831 (2014) 38.
29. C.A. Razzino, L.F. Sgobbi, T.C. Canevari, J. Cancino and S.A.S. Machado, *Food Chem.*, 170 (2015) 360.
30. Y. Yu, C. Jiang, L. Mo, T. Li, L. Xie, J. He, L. Tang, D. Ning and F. Yan, *Food Anal. Methods*, (2016) 1.
31. M. Erami, *Journal of Materials & Environmental Science*, 5 (2014) 1565.
32. R. Cui, D. Xu, X. Xie, Y. Yi, Y. Quan, M. Zhou, J. Gong, Z. Han and G. Zhang, *Food Chem.*, 221 (2016) 457.
33. P. Noyrod, O. Chailapakul, W. Wonsawat and S. Chuanuwatanakul, *J. Electroanal. Chem.*, 719

(2014) 54.

34. S. Luo, Y. Wu and H. Gou, *Ionics*, 19 (2013) 673.

© 2017 The Authors. Published by ESG ([www.electrochemsci.org](http://www.electrochemsci.org)). This article is an open access article distributed under the terms and conditions of the Creative Commons Attribution license (<http://creativecommons.org/licenses/by/4.0/>).